NEACRP-L- 206

Application of the Finite Element Method to the Three-Dimensional Neutron Diffusion Equation

Paper submitted to the NEACRP 21th Meeting

Tokai, November 1978

Takeharu ISE, Toshio YAMAZAKI* and Yasuaki NAKAHARA

Japan Atomic Energy Research Institute

* Sumitomo Heavy Industries, Ltd.

Application of the Finite Element Method to the Three-Dimensional Neutron Diffusion Equation

Takeharu ISE*, Toshio YAMAZAKI** and Yasuaki NAKAHARA

Tokai Research Establishment, Japan Atomic Energy Research Institute

Tokai-mura, Naga-gun, Ibaraki-ken, Japan

Abstract

The finite element method (FEM) was applied to the solution of three-dimensional neutron diffusion equation in order to get a profit from the geometrical flexibility of the FEM.

To circumvent the computer limitations arising from the three-dimensional problem, newly developed program (FEM-BABEL) has been equipped with the following features: Combination of prism- and box-formed finite elements, the SOR method applied successively to x-y planar unit, accelerations of inner iterations by the coarse mesh rebalancing technique and of outer iterations by the SOR extrapolation and the auxiliary program producing mesh network.

Comparisons are made with the conventional finite difference CITATION by solving an analytical solvable problem, a coupled reactor and a pressurized water reactor. Results have shown that the present finite element method has advantages over the finite difference method for solving realistic three-dimensional problems in view of preciseness and computing cost.

---

* Present address: Japan Nuclear Ship Development Agency, Torano-mon, Minato-ku, Tokyo

** Sumitomo Heavy Industries, Ltd., Ohte-machi, Chiyoda-ku, Tokyo

1. Introduction

The finite element method (FEM)[1] has recently been shown to offer attractive solution procedure for neutron diffusion[2~7] and transport problems[2,8~11] as well as structure analysis.[12] One of the most advantages is that FEM can fit precisely to any complicated geometry (geometrical flexibility). We therefore have investigated the applicability of FEM to the numerical solution of the multigroup neutron diffusion equation for the three-dimensional reactor configuration.

Three-dimensional diffusion calculation is the most practical way to take into account all the essential features of realistic nuclear design problems. Among various kinds of three-dimensional elements like tetrahedron, hexahedron, quadrilateral prism, triangular prism (prism shape), rectangular prism (box shape) and so on,[13] the prism- or box-shaped element is considered to be most appropriate for describe the reactor geometry from the viewpoint of preciseness and computer economy in balance. This is a reason why we adopt FEM having the prism- and box-shaped elements in order to analyze a practical problem.

However one must pay two penalties for these advantages; One is that a million unknowns may be needed to solve accurately the system equations for realistic three-dimensional problems. Moreover the coefficient matrices have sparse and irregular structure. Another is that the program user must specify a large amount of input data inherent in FEM. Thus in our newly developed program (FEM-BABEL)[7] we have adopted the iterative method (successive over-relaxation method)[14] for paying the former penalty and we have produced the finite element mesh generator[15] as an auxiliary program for the latter.

The verification and applicability of the program have been demonstrated by solving the exact problem, a coupled core reactor and a pressurized

water reactor in comparison with the conventional finite difference calculations (CITATION).[16]

2. Solution of the Neutron Diffusion Equation by the Finite Element Method

In the general multigroup formalism, the neutron diffusion equation is represented by a coupled system of differential equations on the scalar flux ϕ,

$$-\nabla D_g(r)\nabla\phi_g(r) + \Sigma_{r,g}(r)\phi_g(r) = \frac{\chi_g}{K_{eff}} \sum_{g'=1}^{G} (\nu\Sigma_f)_{g'}(r)\phi_g(r)$$

$$+ \sum_{\substack{g'=1 \\ (g'<g)}}^{G} \Sigma_{s,g'g}(r)\phi_{g'}(r), \quad g=1,2,\ldots,G \quad \text{for } r \in \Omega \qquad (1)$$

where the notation is conventional.

By denoting the external boundary of a domain Ω by $\partial_e\Omega$, Eq. (1) should satisfy the general form of boundary condition:

$$a(r)D_g\left(\frac{\partial\phi_g}{\partial n}\right)(r) + b(r)\phi_g(r) = 0 , \qquad r \in \partial_e\Omega \qquad (2)$$

where $\partial/\partial n$ represents the outward normal derivative at $\partial_e\Omega$ with unit vector n. In applying the finite element method, the domain Ω is assumed the union of a finite number N of contiguous small subdomain Ω_i which is called the finite element hereafter,

$$\Omega = \bigcup_{i=1}^{N} \Omega_i \ .$$

If the subdomain possesses the interface $\partial_i\Omega$, then Eq. (1) requires the usual interface conditions with respect to neutron flux and current:

$$\phi_g(r) \text{ and } \left(D_g \frac{\partial\phi}{\partial n}\right)(r) \text{ are continuous across } \partial_i\Omega. \qquad (3)$$

Now to solve the generalized eigenvalue problem described by Eqs. (1) - (3) for K_{eff} and the corresponding positive eigenfunction $\{\phi_g(r)\}$, we adopt the usual outer iteration procedure. At each step of this outer iteration, we thus solve G uncoupled self-adjoint elliptic boundary value problems of the matrix form (n: iterated index):

$$[-\nabla D(r)\nabla + \Sigma(r)]\,\phi^{(n)}(r) = F^{(n-1)}(r)\ , \tag{4}$$

where

$$F^{(n-1)}(r) = \frac{1}{K_{eff}^{(n-1)}}\,\chi(r)S(r)\phi^{(n-1)}(r),$$

$$\Sigma = \Sigma_r - \Sigma^d\ ,$$

$$\Sigma_r = \mathrm{diag}[\Sigma_{r,g}]\ ,$$

$$D = \mathrm{diag}[D_g],$$

$$\Sigma^d = \begin{bmatrix} 0 & & & 0 \\ \Sigma_{s,12} & 0 & & \\ \Sigma_{s,13} & \Sigma_{s,23} & 0 & \\ \vdots & \vdots & & \\ \Sigma_{s,1G} & & \Sigma_{s,G-1,G} & 0 \end{bmatrix}\ ,$$

$$\chi = \mathrm{col}\,\{\chi_g\}\ ,$$

$$S = \mathrm{col}\,\{\nu\Sigma_{f,g}\}\ ,$$

$$\phi = \mathrm{col}\,\{\phi_g\}\ .$$

The conservation of the self-adjoint character provides the Galerkin-type approximation procedure for the numerical solution of the elliptic boundary value problem.[4]

Here we define the Galerkin-type approximation to the present problem. Lt $W_2^1(\Omega)$ be Sobolev space, the weak form of the original problem is given by

$$a(\phi,\psi) = (F,\psi) \qquad \text{for all } \psi \in W_2^1(\Omega)\ , \tag{5}$$

where

$$a(\phi,\psi) = \int_\Omega [D\nabla\phi\nabla\psi + \Sigma\phi\psi]dV + \int_{\partial e'\Omega} \frac{b}{a}\phi\psi dS \ ,$$

$$\partial e'\Omega = \{r | r \in \partial_e\Omega,\ a(r) > 0\}$$

and

$$(F,\psi) = \int_\Omega F\psi dV$$

Let M_N be any finite-dimensional subspace $W_2^1(\Omega)$, then our aim is to solve the approximate problem having a unique solution $\hat{\phi}$ in M_N,

$$a(\hat{\phi},\psi) = (F,\psi) \qquad \text{for all } \psi(r) \in M_N \ . \tag{6}$$

In order to uniquely determine $\hat{\phi} \in M_N$, we have chosen linear Lagrange polynomials which we take the reference points at the nodes of grid over the subdomain. Since we associate one degree of freedom with each node, the dimension of the finite-dimensional subspace M_N is precisely N or the total number of nodes in Ω.

We now associate with each node (global index i) in Ω a basis u_i which possesses the minimum support. That is, u_i vanishes outside the union of the finite element to which the i-th node belongs. Futhermore u_i takes the value 1 at the i-th node and the value 0 at all other nodes within its support. Then the solution $\hat{\phi}$ of the approximate problem Eq. (6) will be of the form

$$\hat{\phi}_g(r) = \sum_{i=1}^{N} q_{gi}u_i \ , \tag{7}$$

where $\{u_i\}$ is the basis of the space M_N to be constructed and the coefficient $\{q_{gi}\}$ represents the value of $\hat{\phi}$ at the node. In other words, we have the identity:

$$\hat{\phi}_g(r_i) = q_{gi} \ , \qquad \text{for } i = 1, 2, \ldots, N \ . \tag{8}$$

Our goal is now to determine the basis u in terms of the nodal parameter q (q is the generalized coordinate in the finite element terminology).

Substituting Eq. (7) into Eq. (6) and taking successively each of the basis functions of M_N for ψ, we obtain a linear system of equations:

$$\sum_{j=1}^{N} q_{gi}\, a(u_j,u_i) = (F,u_i), \quad i = 1, 2, \ldots\ldots, N , \tag{9}$$

from which the unknown nodal parameter q can be solved. This approximate approach is commonly referred to as the finite element method.

We now consider a partition Ω into prism- and box-shaped subdomains. The union of these subdomains is arbitrary except the restriction that every portion of any material interface lies on an edge of a subdomain. It is observed that the bilinear form $a(u_i,u_j)$ is non-zero only if the subdomain of u_i and u_j possesses at least one subdomain in common. Denote by Γ_{ij} the set of indices (γ) of these subdomains (T_γ) which belong to the intersection of the subdomains of u_i and u_j. Then we obtain

$$a(u_i,u_j) = \sum_{\gamma\varepsilon\Gamma_{ij}} a^{\gamma}(u_i,u_j), \tag{10}$$

where $a^{\gamma}(u_i,u_j)$ is the integral of Eq. (6) over the subdomain T_γ. Using Eq. (10), we obtain the following equation on the subdomain T_γ corresponding to Eq. (7):

$$\hat{\phi}^{\gamma} = q^{\gamma}\, u^{\gamma} \tag{11}$$

3. Description of the Computer Program

Since we have chosen prism- and box-shaped elements, the basis function may be partitioned into axial and planar components:

$$u(x,y,z) = f(z)\cdot u(x,y) . \tag{12}$$

Then the Galerkin approximation derived in the previous section leads to

the system equation to be solved as follows:

$$[H]^g\{\phi\}^g = \{S\}^g , \qquad \text{for } g = 1, 2, \ldots, G, \tag{13}$$

where

$$[H] = D^g[Q]^\gamma + \Sigma_r^g[B]^\gamma, \tag{13.1}$$

$$S = \frac{\chi^g}{K_{eff}} \sum_{g'} [F]^{\gamma,g'} \phi^{g'} + \sum_{g'} [K]^{\gamma,g'g} \phi^{g'} ,$$

in which

$$[F]^{\gamma,g'} = (\nu\Sigma_f)^{g'}[B]^\gamma , \tag{13.2}$$

$$[K]^{\gamma,g'g} = \Sigma_s^{g'g}[B]^\gamma , \tag{13.3}$$

and γ is the superscript which denotes the prism- or box-shaped element. The $[Q]^\gamma$ and $[B]^\gamma$ are the integrals over finite elements:

$$\begin{aligned} Q_{ij}^\gamma &= \int \nabla u_i(x,y,z) \cdot \nabla u_j(x,y,z)\,dxdydz \\ B_{ij}^\gamma &= \int u_i(x,y,z) \cdot u_j(x,y,z)\,dxdydz \end{aligned} \tag{14}$$

Accordingly the three-dimensional $[Q]^\gamma$ and $[B]^\gamma$ may be expressed by using the two-dimensional ones as follows.

Let I and II be the planar indices over elements as shown in Fig. 1. Then the matrices contained in Eq. (13) are written by the submatrices having planar indices as follows:

$$[H] = \begin{pmatrix} A_I & C_I \\ C_I & A_{II} \end{pmatrix} , \tag{15}$$

$$[F] = \begin{pmatrix} F_I & G_I \\ G_I & F_{II} \end{pmatrix} , \tag{15.1}$$

$$[K] = \begin{pmatrix} S_I & R_I \\ R_I & S_{II} \end{pmatrix} , \tag{15.2}$$

and

$$[Q]^{\gamma} = \begin{pmatrix} Q_I & P_I \\ P_I & Q_I \end{pmatrix} , \tag{15.3}$$

$$[B]^{\gamma} = \begin{pmatrix} B_I & D_I \\ D_I & B_I \end{pmatrix} , \tag{15.4}$$

where

$$A_I = A_{II} = DQ_I + \Sigma_r B_I , \tag{15.5}$$

$$C_I = DP_I + \Sigma_r D_I , \tag{15.6}$$

$$F_I = F_{II} = (\nu\Sigma_f)B_I , \tag{15.7}$$

$$G_I = (\nu\Sigma_f)D_I , \tag{15.8}$$

$$S_I = S_{II} = \Sigma_s B_I , \tag{15.9}$$

$$R_I = \Sigma_s D_I , \tag{15.10}$$

In addition, Q_I, P_I, B_I and D_I are expressed by two-dimensional submatrices:

$$P_I = \Delta z Q^{\gamma(2)} - \frac{1}{\Delta z} B^{\gamma(2)} , \tag{15.11}$$

$$Q_I = 2\Delta z Q^{\gamma(2)} + \frac{1}{\Delta z} B^{\gamma(2)} ,$$

$$B_I = 2D_I , \tag{15.13}$$

$$D_I = \frac{1}{6} \Delta z B^{\gamma(2)} , \tag{15.14}$$

where $Q^{\gamma(2)}$ and $B^{\gamma(2)}$ are two-dimensional Q^{γ} and B^{γ}, respectively. In other words, $Q^{\gamma(2)}$ and $B^{\gamma(2)}$ correspond to triangular and rectangular elements which have already shown in the appendix of Reference 7 for detail or in Reference 3.

Our ultimate object is to solve Eq. (13). Since the global matrix [H] possesses the tridiagonal structure which is composed of planar submatrices, Eq. (13) is solved by the successive over-relaxation method (SOR)[14] in which the inner iterations are successively performed within

the core memory for each planar layer. This planar-like SOR will give a large help from the viewpoint of less storage limitations to computers.

The inner iterations are accelerated by means of the coarse mesh rebalancing technique[17] and the outer iterations by means of the extrapolation based on SOR. The program is all written in the FORTRAN-IV language implementing on the FACOM 230/75 operating system, equipped with the free field FIDO format, the complete restarting procedure, the automatic mesh generator built in for a regular mesh network, and the auxiliary mesh generator with half of the graphic display for a pressurized water reactor.

4. Numerical Tests and Results

In this section, we present the results of a detailed comparison study of the three-dimensional finite element calculations for the numerical solution of the neutron diffusion equation to show the reliability of the computer program FEM-BABEL. The comparisons are made for preciseness and computing cost of the eigenvalues and the eigenfuctions between the finite element program FEM-BABEL and the finite difference program CITATION. For this purpose the numerical tests refer to the three different types of reactor configurations: a homogeneous cubic reactor problem which is exactly solvable (an exact problem), a simplified two-zone reactor with two energy groups (a coupled reactor problem), and a little modified IAEA three-dimensional benchmark problem (a pressurized water reactor problem). Material constants for the test problems are referred to Reference 4 for both the exact problem and the coupled reactor problem and to Reference 6 for the pressurized water reactor problem.

To verify the computer program, it will be best to deal with the analytically solvable problem for a homogeneous cubic reactor in a two-energy-group model. The reactor configuration is illustrated in Fig. 2.

For program check of FEM-BABEL, we have used both this exact solution and the finite difference solution. Tables 1 and 2 show that the present finite element program gives precise solutions for both eigenvalues (K_{eff}) and eigenfunctions (fluxes). It is noted that the exact eigenvalue lies between the finite element and the finite difference solutions. It is shown in Table 3 that the finite element calculations have the advantage of computing cost over the finite difference calculations.

As shown in Fig. 3, the coupled reactor configuration will provide saddle shaped neutron flux distributions. Such flux behaviors are substantially different from those in another reactors. Since this configuration is symmetric with respect to the two diagonals (the 45-deg symmetry), the present finite element program can take advantage of this symmetry by use of both prism- and box-shaped elements. Table 4 shows that the finite element solutions are in an excellent agreement with the reference value (from experience for the exact problem we take as the reference value the average of the two numerical solutions for the mesh size of 2.5 cm). It is shown in Fig. 4 that both the numerical solutions are in a good agreement on the flux distribution. Table 5 shows that the finite element calculations have an advantage of computing cost over the finite difference also for a coupled reactor.

Finally we discuss the efficiency of the program for a real scale pressurized water reactor illustrated in Fig. 5. This problem comes from a slight modification of the IAEA water reactor problem for reason of consistency to the boundary condition of the finite difference calculation. That is, discussion is performed on the octant reactor configuration in the finite element calculations but on the quarter reactor configuration in the finite difference calculations. The mesh size are taken 5 cm on x-y plane and 10 cm in Z direction.

Figures 6 and 7 illustrate comparisons of radial power distributions and axial power distributions, respectively. It is likely that the finite element solutions show a better performance than the finite difference solutions especially near the core-reflector interface. Table 6 lists comparison of outer iterative performance and Table 7 comparison of the solution techniques. The results show that the finite element solutions take advantage over the finite difference solutions about the iterative performance and the storage requirements, but disadvantage about the computing time because of difference between the solution techniques on data processing.

5. Conclusions

Through both the analytical and numerical ~~problems~~ tests, it may be concluded that the three-dimensional finite element calculations are acceptable from viewpoints of preciseness and computing cost. It is seen that the iterative method adopted is effective, too. It is noted that in the present tests we do not use the coarse mesh rebalancing accelerations built in the program (it is reported that the acceleration is very effective for a practical problem[18]). By using this technique the computing time will be reduced to some extent compared to the present calculation. Now an improvement to the iterative method is tried by one in our laboratory. The auxiliary program on finite element mesh generation already developed by us will give the users a help to prepare a large amount of data.

References

1) Strang G. and Fix G.J.: "Analysis of the Finite Element Method," Prentice-Hall (1971)

2) Ohnishi T.: "Application of the Finite Element Solution Techniques to

Neutron Diffusion and Transport Equations," CONF-710302, Vol.II, 273 (1971)

3) Semenza L.A., Lewis E.E. and Rossow E.C.: "The application of the finite element method to the multigroup neutron diffusion equation," Nucl. Sci. Eng., 47, 302 (1972)

4) Kaper H.G., Leaf G.K. and Lindeman A.J.: "A timing comparison study for some high order finite element approximation procedures and a low order finite difference approximation procedures for the numerical solution of the multigroup neutron diffusion equation," Nucl. Sci. Eng., 49, 27 (1972)

5) Kang C.M. and Hansen K.F.: "Finite element methods for space-time reactor analysis," Nucl. Sci., Eng., 51, 456 (1973)

6) Misfeldt I.: "Solution of the Multigroup Neutron Diffusion Equations by the Finite Element Method," RISO-M-1809 (1975)

7) Ise T., Yamazaki T. and Nakahara Y.: "FEM-BABEL, a Computer Program for Solving Three-Dimensional Neutron Diffusion Equation by the Finite Element Method," JAERI-1256 (1978)

8) Reed W.H., Hill T.R., Brinkley F.W. and Lathrop K.D.: "TRIPLET: a Two-Dimensional, Multigroup, Triangular Mesh, Planar Geometry, Explicit Transport Code," LA-5428-MS (1973)

9) Lewis E.E., Miller Jr. W.F. and Henry T.P.: "A two-dimensional finite element method for integral neutron transport calculations," Nucl. Sci. Eng., 58, 203 (1975)

10) Martin W.R. and Duderstadt J.J.: "Finite element solutions of the neutron transport equation with applications to strong heterogeneities," Nucl. Sci. Eng., 62, 371 (1977)

11) Fujimura T., Tsutsui T., Horikami K., Nakahara Y. and Ohnishi T.: "Application of finite element method to two-dimensional multi-group

neutron transport equation in cylindrical geometry," J. Nucl. Sci. Technol., 14, 541 (1977)

12) Zienkiewicz O.C.: "The Finite Element Method in Engineering and Science," McGraw-Hill (1971)

13) Desai C.S. and Abel J.F.: "Introduction to the Finite Element Method," Van Nostrand (1972)

14) Varga R.A.: "Matrix Iterative Analysis," Prentice-Hall (1962)

15) Ise T. and Yamazaki T.: "LOOM-P, a Finite Element Mesh Generator Program with On-Line Graphic Display," JAERI-M 7119 (1977)

16) Fowler T.B., Vondy D.R. and Cunningham G.W.: "Nuclear Reactor Core Analysis Code: CITATION," ORNL-TM-2496, Rev. 2 (1971)

17) Freolich R.: "A Theoretical Foundation for Coarse Mesh Variational Techniques," Intern. Conf. Research Reactor Utilization and Reactor Mathematics, Mexico, 219 (1967)

18) Freolich R.: "Flux Synthesis Methods versus Difference Approximation Methods for the Efficient Determination of Neutron Flux Distributions in Fast and Thermal Reactors," IAEA-SM-154/14 in "Numerical Reactor Calculations," IAEA (1972)

Table 1 Comparison of the multiplication factors between the numerical and analytical solutions for the exact problem

Analytical solution	Numerical solution		Mesh size (cm)					
			2		5		10	
			K_{eff}	Relative error	K_{eff}	Relative error	K_{eff}	Relative error
1,335506	FEM-BABEL	Quarter	—	—	1.33478	0.054 %	—	—
		Octant	1.33537	0,010 %	1.33473	0,058 %	1,33211	0.25 %
	CITATION		1,33562	0,009 %	1,33623	0.054 %	1.33842	0.22 %

%/

Table 2 Comparison of the second energy group flux $\phi_2(x,0,0)$ at the mesh size of 5 cm for the exact problem

x (cm)		2.5	12.5	22.5	32.5	42.5
Analytical		1.5643	1.4497	1.1932	0.81990	0.36632
FEM-BABEL	Quarter	1.5644	1.4497	1.1932	0.81989	0.36631
	Octant	1.5662	1.4493	1.1929	0.81973	0.36625
CITATION		1.5641	1.4496	1.1933	0.81996	0.36631

Table 3 Comparison of storage requirements and computation times between two numerical calculations for the exact problem

Numerical method		Mesh size (cm)					
		2		5		10	
		Storage (words)	CPU time (sec)	Storage (words)	CPU time (sec)	Storage (words)	CPU time (sec)
FEM-BABEL	Quarter	—	—	10337	54	—	—
	Octant	50669	1775	5594	92	1469	10
CITATION		158585	342	15228	38	4709	25

Table 4 Comparison of multiplication factor between two numerical solutions for the coupled reactor problem

Numerical method		Mesh size: Δx(cm) × Δy(cm) × Δz(cm)		
		2.5×2.5×2.5	2.5×2.5×5.0	5.0×5.0×5.0
FEM-BABEL	Full	——	——	0.978115 (0.48%)
	45° symmetry	0.981742 (0.11%)*	0.971605 (0.12%)	0.977697 (0.52%)
CITATION		0.983884 (0.11%)	0.984248 (0.15%)	0.990954 (0.83%)

* Percents in parentheses show the relative error to the reference value which is the average of the multiplication factors by both the programs for the mesh size of 2.5 cm.

Table 5 Comparison of computing cost between two numerical solutions for the coupled reactor problem

Numerical method		Mesh size: Δx(cm) × Δy(cm) × Δz(cm)					
		2.5×2.5×2.5		2.5×2.5×5.0		5.0×5.0×5.0	
		Storage (words)	CPU time (min.)	Storage (words)	CPU time (min.)	Storage (words)	CPU time (min.)
FEM-BEBEL	Full	——	——	——	——	53188	16.4
	45° symmetry	63313	36.3	53807	18.7	11177	2.6
CITATION		452511	49.5	227391	11.4	57631	2.7

Table 6 Comparison of the iterative performance for the IAEA problem

		FEM-BABEL	CITATION
10th outer iteration	K_{eff}	1.02261(0.58%)*)	1.02075(0.76%)*)
	Outer error	4.5×10^{-4}	7.4×10^{-4}
	Inner error	4.7	3.4×10^{-1}
20th outer iteration	K_{eff}	1.02510(0.34%)	1.02416(0.43%)
	Outer error	1.6×10^{-4}	2.2×10^{-4}
	Inner error	3.5×10^{-2}	1.6×10^{-1}
30th outer iteration	K_{eff}	1.02635(0.22%)	1.02572(0.28%)
	Outer error	9.6×10^{-5}	1.2×10^{-4}
	Inner error	2.5×10^{-2}	2.7×10^{-1}
34th outer iteration	K_{eff}	1.02670(0.19%)	1.02614(0.24%)
	Outer error	8.0×10^{-5}	9.7×10^{-5}
	Inner error	2.2×10^{-5}	1.6×10^{-2}

*) Reference value is the CITATION result of K_{eff} = 1.028615, with outer error of $1.\times10^{-6}$ and inner error of $6.\times10^{-4}$, at 63th outer iteration.

Table 7 Comparison of the solution techniques and the computing costs for the IAEA problem

	FEM-BABEL	CITATION
Program size	41 kilowords	61 kilowords
Solution method	use only SOR but not coarse mesh rebalancing	SOR with adaptive extrapolation
Acceleration for outer iterations	fixed extrapolation by SOR with $\beta_s = 1.7$	Chebyshev extrapolation
Storage requirements and data processing	126 kilowords; with only planar data in memory	455 kilowords; with all data in core memory
CPU time at the same outer error of 0.24%	120 min. for 28 outer iterations	32 min. for 34 outer iterations

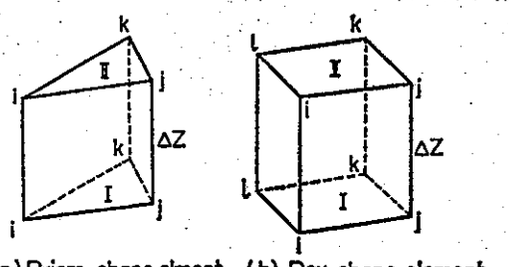

Fig. 1 Local node indices on x-y planar layers for both the finite elements

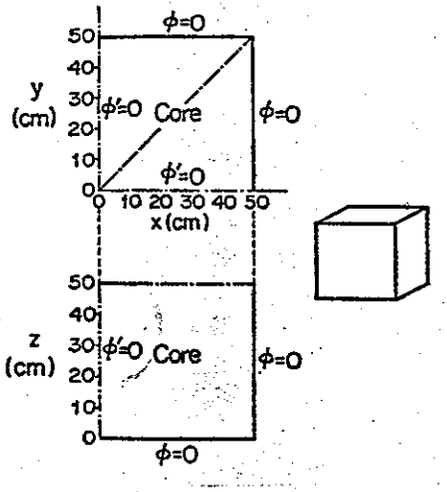

Fig. 2 Reactor configuration for the exact problem

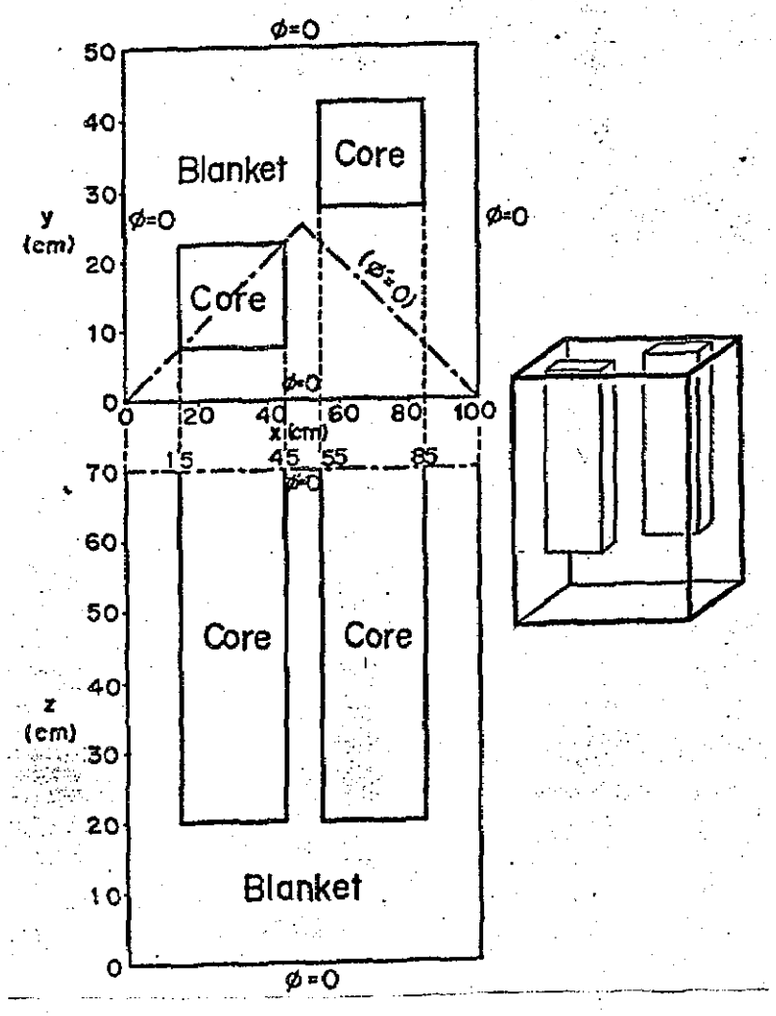

Fig. 3 Coupled reactor configuration

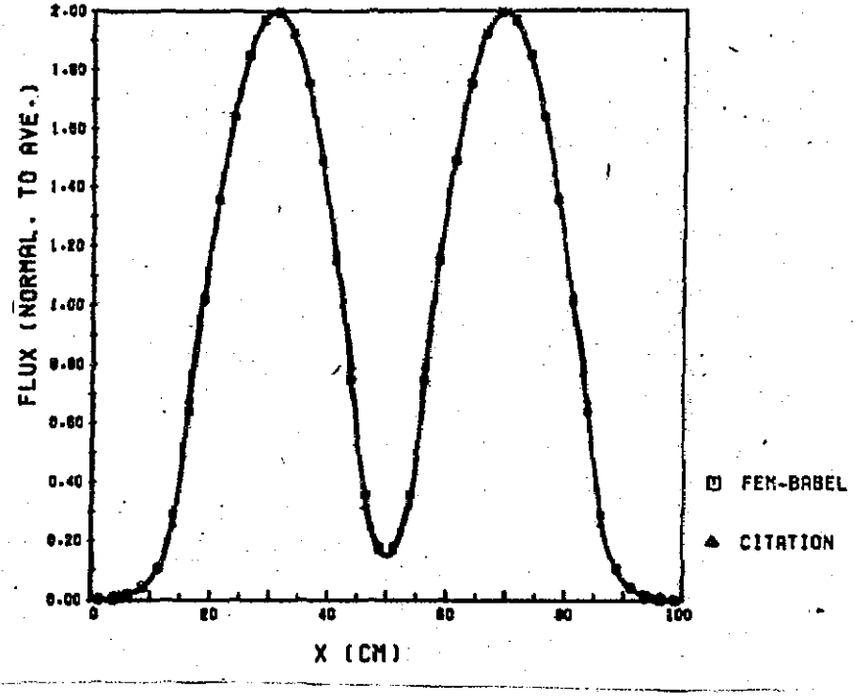

Fig. 4 Comparison of fast flux distributions for the coupled reactor problem

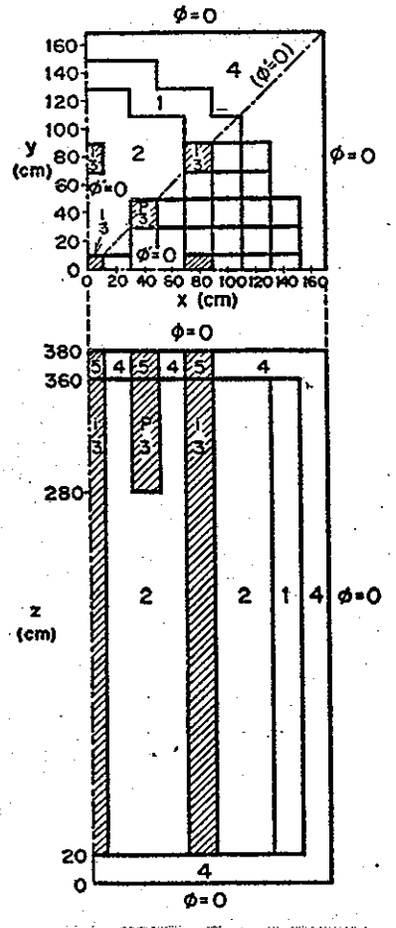

Fig. 5 Reactor configuration of the IAEA problem

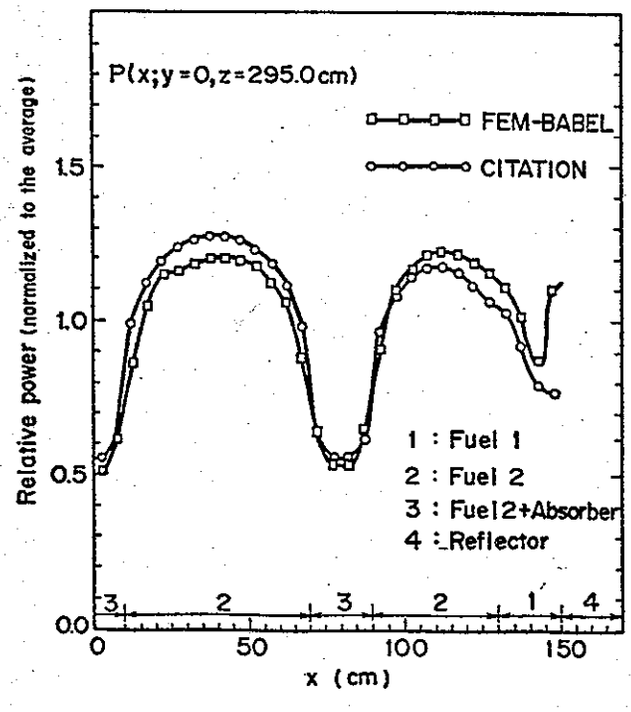

Fig. 6 Comparison of radial power distributions for the IAEA problem

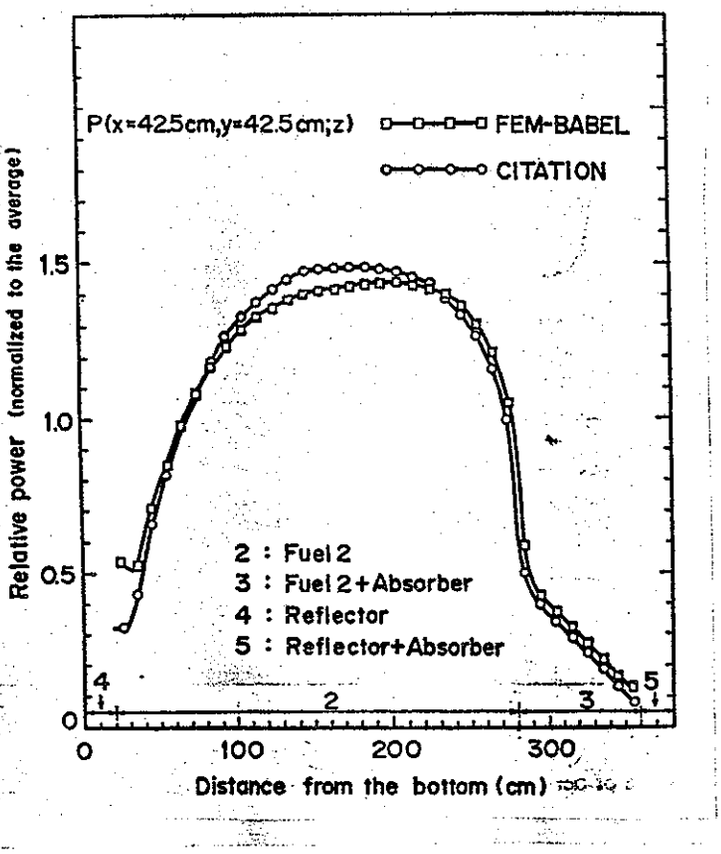

Fig. 7 Comparison of axial power distributions for the IAEA problem